The Astrophysical Journal, 692:L29–L33, 2009 February 10 doi:10.1088/0004-637X/692/1/L29

DISCOVERY OF A VERY HIGH ENERGY GAMMA-RAY SIGNAL FROM THE 3C 66A/B REGION

E. Aliu[1], H. Anderhub[2], L. A. Antonelli[3], P. Antoranz[4], M. Backes[5], C. Baixeras[6], S. Balestra[4], J. A. Barrio[4], H. Bartko[7], D. Bastieri[8], J. Becerra González[9], J. K. Becker[5], W. Bednarek[10], K. Berger[10], E. Bernardini[11], A. Biland[2], R. K. Bock[7,8], G. Bonnoli[12], P. Bordas[13], D. Borla Tridon[7], V. Bosch-Ramon[13], T. Bretz[14], I. Britvitch[2], M. Camara[4], E. Carmona[7], A. Chilingarian[15], S. Commichau[2], J. L. Contreras[4], J. Cortina[1], M. T. Costado[9,16], S. Covino[3], V. Curtef[5], F. Dazzi[8], A. De Angelis[17], E. De Cea del Pozo[18], R. de los Reyes[4], B. De Lotto[17], M. De Maria[17], F. De Sabata[17], C. Delgado Mendez[9], A. Dominguez[19], D. Dorner[2], M. Doro[8], D. Elsaesser[14], M. Errando[1,27], D. Ferenc[20], E. Fernández[1], R. Firpo[1], M. V. Fonseca[4], L. Font[6], N. Galante[7], R. J. García López[9,16], M. Garczarczyk[7], M. Gaug[9], F. Goebel[7,28], D. Hadasch[5], M. Hayashida[7], A. Herrero[9,16], D. Höhne-Mönch[14], J. Hose[7], C. C. Hsu[7], S. Huber[14], T. Jogler[7], D. Kranich[2], A. La Barbera[3], A. Laille[20], E. Leonardo[12], E. Lindfors[21,27], S. Lombardi[8], F. Longo[17], M. López[8], E. Lorenz[2,7], P. Majumdar[11], G. Maneva[22], N. Mankuzhiyil[17], K. Mannheim[14], L. Maraschi[3], M. Mariotti[8], M. Martínez[1], D. Mazin[1,27], M. Meucci[12], M. Meyer[14], J. M. Miranda[4], R. Mirzoyan[7], J. Moldón[13], M. Moles[19], A. Moralejo[1], D. Nieto[4], K. Nilsson[21], J. Ninkovic[7], N. Otte[7,23,29], I. Oya[4], R. Paoletti[12], J. M. Paredes[13], M. Pasanen[21], D. Pascoli[8], F. Pauss[2], R. G. Pegna[12], M. A. Perez-Torres[19], M. Persic[17,24], L. Peruzzo[8], F. Prada[19], E. Prandini[8], N. Puchades[1], A. Raymers[15], W. Rhode[5], M. Ribó[13], J. Rico[1,25], M. Rissi[2], A. Robert[6], S. Rügamer[14], A. Saggion[8], T. Y. Saito[7], M. Salvati[3], M. Sanchez-Conde[19], P. Sartori[8], K. Satalecka[11], V. Scalzotto[8], V. Scapin[17], T. Schweizer[7], M. Shayduk[7], K. Shinozaki[7], S. N. Shore[26], N. Sidro[1], A. Sierpowska-Bartosik[18], A. Sillanpää[21], J. Sitarek[7,10], D. Sobczynska[10], F. Spanier[14], A. Stamerra[12], L. S. Stark[2], L. Takalo[21], F. Tavecchio[3], P. Temnikov[22], D. Tescaro[1], M. Teshima[7], M. Tluczykont[11], D. F. Torres[18,25], N. Turini[12], H. Vankov[22], A. Venturini[8], V. Vitale[17], R. M. Wagner[7], W. Wittek[7], V. Zabalza[13], F. Zandanel[19], R. Zanin[1], and J. Zapatero[6]

[1] IFAE, Edifici Cn., Campus UAB, E-08193 Bellaterra, Spain
[2] ETH Zurich, CH-8093 Switzerland
[3] INAF National Institute for Astrophysics, I-00136 Rome, Italy
[4] Universidad Complutense, E-28040 Madrid, Spain
[5] Technische Universität Dortmund, D-44221 Dortmund, Germany
[6] Universitat Autònoma de Barcelona, E-08193 Bellaterra, Spain
[7] Max-Planck-Institut für Physik, D-80805 München, Germany
[8] Università di Padova and INFN, I-35131 Padova, Italy
[9] Instituto de Astrofísica de Canarias, E-38200 La Laguna, Tenerife, Spain
[10] University of Łódź, PL-90236 Lodz, Poland
[11] Deutsches Elektronen-Synchrotron (DESY), D-15738 Zeuthen, Germany
[12] Università di Siena, and INFN Pisa, I-53100 Siena, Italy
[13] Universitat de Barcelona (ICC/IEEC), E-08028 Barcelona, Spain
[14] Universität Würzburg, D-97074 Würzburg, Germany
[15] Yerevan Physics Institute, AM-375036 Yerevan, Armenia
[16] Departamento de Astrofísica, Universidad, E-38206 La Laguna, Tenerife, Spain
[17] Università di Udine, and INFN Trieste, I-33100 Udine, Italy
[18] Institut de Cienciès de l'Espai (IEEC-CSIC), E-08193 Bellaterra, Spain
[19] Instituto de Astrofísica de Andalucia (CSIC), E-18080 Granada, Spain
[20] University of California, Davis, CA-95616-8677, USA
[21] Tuorla Observatory, Turku University, FI-21500 Piikkiö, Finland
[22] Institute for Nuclear Research and Nuclear Energy, BG-1784 Sofia, Bulgaria
[23] Humboldt-Universität zu Berlin, D-12489 Berlin, Germany
[24] INAF/Osservatorio Astronomico and INFN, I-34143 Trieste, Italy
[25] ICREA, E-08010 Barcelona, Spain
[26] Università di Pisa, and INFN Pisa, I-56126 Pisa, Italy
Received 2008 October 26; accepted 2008 December 16; published 2009 January 21

ABSTRACT

The MAGIC telescope observed the region around the distant blazar 3C 66A for 54.2 hr in 2007 August–December. The observations resulted in the discovery of a γ-ray source centered at celestial coordinates R.A. $= 2^{\rm h}23^{\rm m}12^{\rm s}$ and decl.$= 43^\circ 0\farcm7$ (MAGIC J0223+430), coinciding with the nearby radio galaxy 3C 66B. A possible association of the excess with the blazar 3C 66A is discussed. The energy spectrum of MAGIC J0223+430 follows a power law with a normalization of $(1.7 \pm 0.3_{\rm stat} \pm 0.6_{\rm syst}) \times 10^{-11}$ TeV^{-1} cm^{-2} s^{-1} at 300 GeV and a photon index $\Gamma = -3.10 \pm 0.31_{\rm stat} \pm 0.2_{\rm syst}$.

Key words: BL Lacertae objects: individual (3C 66A) – galaxies: individual (3C 66B) – gamma rays: observations – ISM: individual (MAGIC J0223+430)

1. INTRODUCTION

As of today, there are 23 known extragalactic very high energy (VHE, defined here as $E > 100$ GeV) γ-ray sources. All of them are active galactic nuclei (AGNs) with relativistic jets. With the exception of the radio galaxy M 87 all detected sources are blazars, whose jets (characterized by a bulk Lorentz factor $\Gamma \sim 20$) point, within a small angle ($\theta \sim 1/\Gamma$), to the observer. The spectral energy distribution (SED, logarithm of the observed energy density versus logarithm of the photon energy) of AGNs typically shows a two-bump structure. The lower-energy bump originates from synchrotron radiation of relativistic electrons spiraling in the magnetic field of the jet. For the origin of the high-frequency bump, various models have been proposed, the most popular invoking inverse Compton scattering of ambient photons. There have been several suggestions for the origin of the low-frequency seed photons that are up-scattered to γ-ray energies: they may be produced within the jet by synchrotron radiation (the synchrotron self-Compton or SSC mechanism, e.g., Maraschi et al. 1992; Bloom & Marscher 1996) or come from outside the jet (the external Compton or EC mechanism, e.g., Dermer & Schlickeiser 1993). Relativistic effects boost the observed emission as the Doppler factor depends on the angle to the line of sight. For sources with a large angle between the jet and the line of sight (e.g., the radio galaxy M 87), these classic inverse Compton scenarios cannot account for the VHE γ-ray emission. In this case, models that depend less critically on beaming effects are needed (e.g., Neronov & Aharonian 2007; Tavecchio & Ghisellini 2008a). The VHE γ-ray emission of AGNs might also be of hadronic origin through the emission from secondary electrons (e.g., Mannheim 1993; Mücke et al. 2003).

3C 66A and 3C 66B are two AGNs separated by just 6′ in the sky. 3C 66B is a large Fanaroff–Riley-I-type (FRI) radio galaxy, similar to M 87, with a redshift of 0.0215 (Stull et al. 1975), whereas 3C 66A is a blazar with uncertain redshift. The often quoted redshift of 0.444 (Miller et al. 1978) for 3C 66A is based on a single measurement of one emission line only (and the authors were not certain on the realness of the feature), while in later observations no lines in the spectra of 3C 66A were reported (Finke et al. 2008). Based on the marginally resolved host galaxy (Wurtz et al. 1996), a photometric redshift of ∼0.321 was inferred.

3C 66A, a promising candidate for VHE γ-ray emission, was observed several times with satellite-borne and ground-based γ-ray detectors. The EGRET source 3EG J0222+4253 was associated with 3C 66A (Hartman et al. 1999), but the association was ambiguous because the error box is large enough to cover 3C 66B and the nearby pulsar PSR J0218+4232 (Verbunt et al. 1996; Kuiper et al. 2000). In the TeV regime the Crimean Astrophysical Observatory's GT-48 imaging atmospheric Cerenkov telescope has claimed repeated detections of this source above 900 GeV (Neshpor et al. 1998; Stepanyan et al. 2002) with a flux as high as $(3 \pm 1) \times 10^{-11}$ cm^{-2} s^{-1}. HEGRA and WHIPPLE reported upper limits, $F(> 630\,\mathrm{GeV}) < 1.42 \times 10^{-11}$ cm^{-2} s^{-1} (Aharonian et al. 2000) and $F(> 350\,\mathrm{GeV}) < 0.59 \times 10^{-11}$ cm^{-2} s^{-1} (Horan et al. 2004), from non-simultaneous observations. The STACEE solar array also provided an upper limit of $F(> 184\,\mathrm{GeV}) < 1.2 \times 10^{-10}$ cm^{-2} s^{-1} (Bramel et al. 2005). In 2008 September, the Veritas collaboration reported a clear detection of 3C 66A (Swordy 2008) above 100 GeV with an integral flux on the level of 10% of the Crab Nebula flux. Shortly after, a high state of 3C 66A was also reported by the Fermi Gamma-ray Space Telescope at energies above 20 MeV (Tosti 2008).

In this paper, we report the discovery of VHE γ-ray emission located 6.′1 away from the blazar 3C 66A and coinciding with the radio galaxy 3C 66B in 2007. In Section 2, we describe the observations and the data analysis chain. The results of the analysis are presented in Section 3 and discussed in Section 4.

2. OBSERVATIONS AND DATA ANALYSIS

3C 66A underwent an optical outburst in 2007 August, as monitored by the Tuorla blazar monitoring program. The outburst triggered VHE γ-ray observations of the source with the MAGIC telescope following the Target of Opportunity program, which had resulted in discoveries of new VHE γ-ray sources in the past (Albert et al. 2006, 2007a; Teshima 2008).

MAGIC has a standard trigger threshold of 60 GeV, an angular resolution of ∼0.°1, and an energy resolution above 150 GeV of ∼25% (see Albert et al. 2008a for details).

Data were taken in the false-source tracking (wobble) mode (Fomin et al. 1994) pointing alternately to two different sky directions, each at 24′ distance from the 3C 66A catalog position. The zenith distance distribution of the data extends from 13° to 35°. Observations were made in 2007 August, September, and December, and lasted 54.2 hr, out of which 45.3 hr passed the quality cuts based on the event rate after image cleaning. An additional cut removed the events with total charge less than 150 photoelectrons (phe) in order to assure a better background rejection.

Just before the start of the observation campaign ∼5% of the mirrors on the telescope were replaced, worsening the optical point-spread function (PSF). As a consequence, a new calibration of the mirror alignment system became necessary, which took place within the observation campaign and improved the PSF again. The sigma of the Gaussian PSF (40% light containment) was measured to be 3.′0 in 2007 August 12–14, 2.′6 in 2007 August 15–26, and 2.′1 in 2007 September and December. To take this into account, data were analyzed separately for each period and the results were combined at the end of the analysis chain. However, the realignment resulted in a mispointing, which was taken care of by a new pointing model (Bretz et al. 2009) applied offline using starguider information (Riegel et al. 2005). Considering the additional uncertainty caused by the offline corrections, we estimate the systematic uncertainty of the pointing accuracy to be 2′ on average. Note that in the case of an optimal pointing model the systematic uncertainty is below 2′, being 1′ on average (Bretz et al. 2009; Albert et al. 2008a).

The data analysis consists of several steps. Initially, a standard calibration of the data (Albert et al. 2008d) is performed. In the next step, an image cleaning procedure is applied using the amplitude and timing information of the calibrated signals. In particular, the arrival times of the photons in core pixels (> 6 phe) are required to be within a time window of 4.5 ns and for boundary pixels (> 3 phe) within a time window of 1.5 ns from a neighboring core pixel. For the surviving pixels of each event image parameters are calculated (Hillas 1985). Using the good time resolution of the recorded signals (∼400 ps), unique

[27] Send offprint requests to M. Errando errando@ifae.es, E. Lindfors elilin@utu.fi, D. Mazin mazin@ifae.es.
[28] Deceased.
[29] Current address: University of California, Santa Cruz, CA 95064, USA.

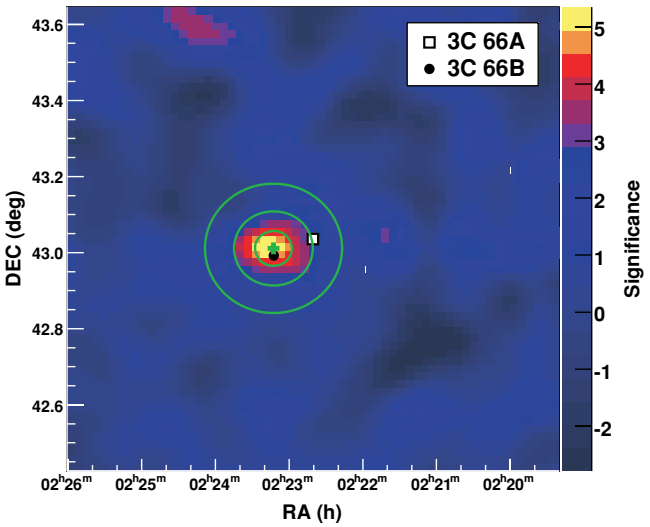

Figure 1. Significance map for γ-like events above 150 GeV in the observed sky region. The green cross corresponds to the fitted maximum excess position of MAGIC J0223+403. The probability of the true source to be inside the green circles is 68.2%, 95.4%, and 99.7% for the inner, middle, and outer contour, respectively. The catalog positions of 3C 66A and 3C 66B are indicated by a white square and a black dot, respectively.

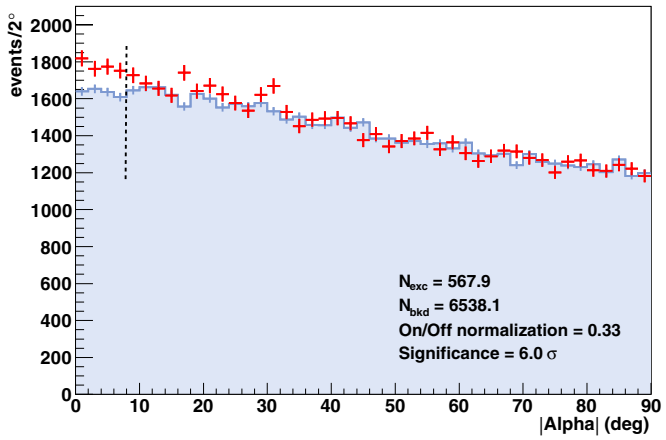

Figure 2. |Alpha| distribution after all cuts evaluated with respect to the position of MAGIC J0223+430. A γ-ray excess with a significance of $6.0\,\sigma$ is found, which corresponds to a post-trial significance of $5.4\,\sigma$.

to MAGIC, the time gradient along the main shower axis and the time spread of the shower pixels are computed (Aliu et al. 2009). Hadronic background suppression is achieved using the Random Forest (RF) method (Albert et al. 2008c), where for each event the so-called Hadronness parameter is computed, based on the image and the time parameters. Moreover, the RF method is used for the energy estimation trained on a Monte Carlo simulated γ-ray sample with the same zenith angle distribution as the data sample.

3. RESULTS

Figure 1 shows a significance map produced from the signal and background maps, both smoothed with a Gaussian of $\sigma = 6'$ (corresponding to the γ-PSF), for photon energies between 150 GeV and 1 TeV. For the background rejection a loose cut in the Hadronness parameter is applied to keep a large number of gamma-like events. The center of gravity of the γ-ray emission is derived from Figure 1 by fitting a bell-shaped function of the form

$$F(x, y) = A \cdot \exp\left[-\frac{(x-\bar{x})^2 + (y-\bar{y})^2}{2\sigma^2}\right] \quad (1)$$

for which the distribution of the excess events is assumed to be rotationally symmetric, i.e., $\sigma_x = \sigma_y = \sigma$. The fit yields reconstructed coordinates of the excess center of R.A. = $2^h23^m12^s$ and decl. = $43°0'.7$. The detected excess, which we name MAGIC J0223+430, is $6'.1$ away from the catalog position of 3C 66A, while the distance to 3C 66B is $1'.1$.

In order to estimate the statistical uncertainty of the reconstructed position, we simulated 10^4 sky maps with the same number of background and excess events as in the data. The excess position in the sky maps was fitted and the distance to the simulated source position calculated. From the histogram of the distances we obtained probabilities for an offset between the true source and the fit to the excess. The probabilities shown in Figure 1 by the green contours correspond to 68.2%, 95.4%, and 99.7% for the inner, middle, and outer contour, respectively. Using this study we found that the measured excess coincides with the catalog position of 3C 66B. The origin of the emission from 3C 66A can be statistically excluded with a probability of 95.6%. Adding linearly the systematic uncertainty of the pointing of the data set ($2'$, see above), i.e., shifting the excess position by $2'$ toward the catalog position of 3C 66A, the exclusion probability is 85.4%.

To calculate the significance of the detection, an |Alpha| distribution was produced, where Alpha is the angle between the major axis of the shower image ellipse and the source position in the camera. For the calculation of the source-dependent image parameters we considered the fitted position of the excess. Background rejection was achieved by a cut in Hadronness, which was optimized using Crab Nebula data taken in similar conditions and diluted to 5% of its real flux. The cut in |Alpha| that defines the signal region was also optimized in the same way. The |Alpha| and Hadronness cuts together have an efficiency of 40% in keeping Monte Carlo simulated γ events, and result in an energy threshold of approximately 230 GeV.[30] A signal of $6.0\,\sigma$ significance (pre-trial) was found (see Figure 2). We estimated the number of trials of the signal search by projecting the γ-ray acceptance of the camera into the field of view of the observations, and defined the search region where the γ-ray acceptance after cuts is larger than 50%. In this way, we obtained an area of 2.18 deg^2. Given that the 68% containment radius for γ-rays from a pointlike source is $0°.152$, we calculated the number of independent trials to be 30.

Figure 3 shows the light curve of MAGIC J0223+430 together with the flux of 3C 66A in optical wavelengths. As we integrate over γ-ray events from a wide sky region ($\sim$0.07 deg^2), we cannot exclude that 3C 66A contributes to the measured signal. The integral flux above 150 GeV corresponds to $(7.3 \pm 1.5) \times 10^{-12}$ cm^{-2} s^{-1} (2.2% of the Crab Nebula flux) and is the lowest ever detected by MAGIC. The γ-ray light curve is consistent with a constant flux within statistical errors. These errors, however, are large, and some variability of the signal cannot be excluded.

For the energy spectrum of MAGIC J0223+430, loose cuts are made to keep the γ-ray acceptance high. The differential energy spectrum was unfolded using the Tikhonov unfolding technique (Tikhonov & Arsenin 1979; Albert et al. 2007b) and is shown in Figure 4. The spectrum can be well fitted by a power

[30] Defined as the peak of the distribution of Monte Carlo generated gamma-ray events after all cuts.

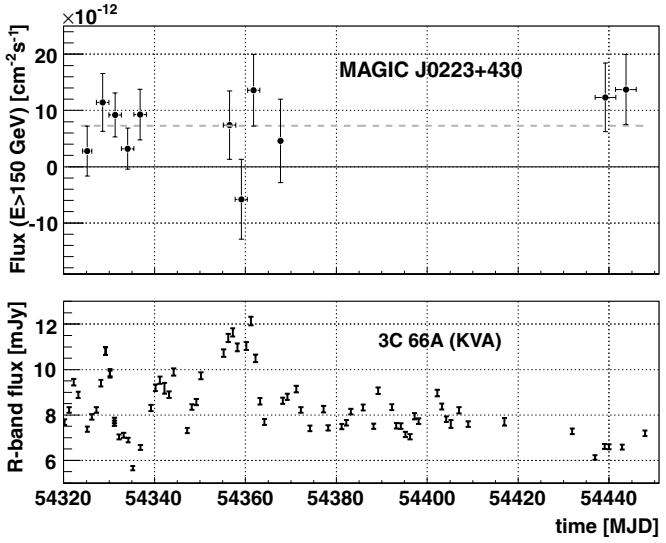

Figure 3. Light curve of MAGIC J0223+430. Upper panel: MAGIC integral flux above 150 GeV in bins of 3 days (except for periods where the sampling was coarser). The gray dashed line indicates the average γ-ray flux. Lower panel: optical light curve of 3C 66A as measured by the KVA telescope. During the MAGIC observations 3C 66A was very bright at optical wavelengths varying from 6 mJy to 12 mJy in the *R*-band (the baseline flux in the historical data being $\sim$ 6 mJy). In the same period the optical flux of 3C 66B remained constant, which is a typical behavior for large radio galaxies.

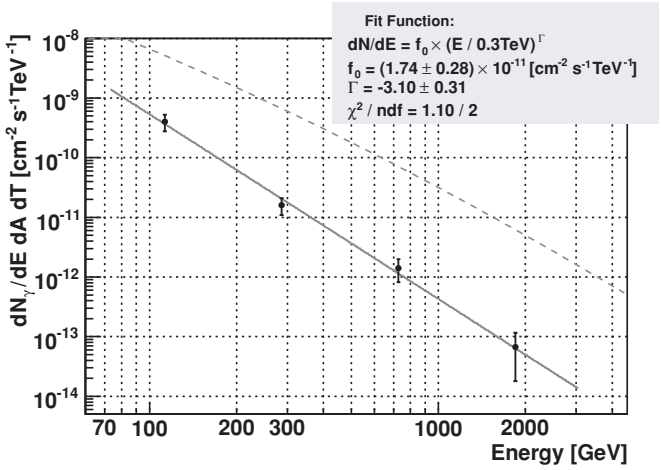

Figure 4. Differential energy spectrum of MAGIC J0223+430. The fit to the data is shown by the solid gray line and the fit parameters are listed in the inset. No correction for the $\gamma - \gamma$ attenuation due to the EBL has been made. The Crab Nebula spectrum (Albert et al. 2008a) is also shown as a reference (dashed gray line).

law which gives a differential flux (TeV^{-1} cm^{-2} s^{-1}) of

$$\frac{dN}{dE\,dA\,dt} = (1.7 \pm 0.3) \times 10^{-11} (E/300\,\mathrm{GeV})^{-3.1\pm0.3}. \quad (2)$$

The quoted errors are statistical only. The systematic uncertainty is estimated to be 35% in the flux level and 0.2 in the power law photon index (Albert et al. 2008a). As in the case of the light curve, we cannot exclude that 3C 66A contributes to the measured signal. Thus, the spectrum shown in Figure 4 represents a combined γ-ray spectrum from the observed region.

4. DISCUSSION AND CONCLUSIONS

A new VHE γ-ray source MAGIC J0223+430 was detected in 2007 August to December. Given the position of the excess measured by MAGIC above 150 GeV, the source of the γ-rays is most likely 3C 66B. The VHE γ-ray flux was found to be on the level of 2.2% Crab Nebula flux and was constant during the observations. The differential spectrum of MAGIC J0223+430 has a photon spectral index of $\Gamma = 3.10 \pm 0.31$ and extends up to $\sim$2 TeV. In view of the recent detection of 3C 66A at VHE γ-rays (Swordy 2008), we note that if 3C 66A was emitting γ-rays in 2007 August to December then its flux was at a significantly lower level than in 2008. We also note that we cannot exclude the scenario suggested in a recent work by Tavecchio & Ghisellini (2008b) that the observed spectrum would be a combination of emission from 3C 66B (dominating at energies above 150 GeV) and blazar 3C 66A (at lower energies).

In the unlikely case, excluded with probability 85.4%, that the total signal and observed spectrum presented in this paper originates from 3C 66A, the redshift of the source is likely to be significantly lower than previously assumed. Due to the energy-dependent absorption of VHE γ-rays with low-energy photons of the extragalactic background (EBL, Gould & Schréder 1967), the VHE γ-ray flux of distant sources is significantly suppressed. We investigated the measured spectrum by MAGIC following the prescription of Mazin & Raue (2007), and derived a redshift upper limit of the source to be $z < 0.17$ ($z < 0.24$) under the assumption that the intrinsic energy spectrum cannot be harder than $\Gamma = 1.5$ ($\Gamma = 0.666$). This assumption of $\Gamma > 1.5$ is based on particle acceleration arguments (Aharonian et al. 2006a), and the fact that none of the sources in the EGRET energy band (not affected by the EBL) has shown a harder spectrum. The latter assumption of $\Gamma > 0.666$ can be considered as an extreme case of the spectrum hardness, suggesting a monochromatic spectrum of electrons when interacting with a soft photon target field (Katarzynski et al. 2006).[31] If $z > 0.24$ for 3C 66A, an alternative explanation for a hard intrinsic spectrum at energies above 100 GeV can be given if γ-rays are passing through a narrow band of optical–infrared photons in the vicinity of the blazar. Such narrow radiation fields can produce arbitrarily hard intrinsic spectra by absorbing specific energies of γ-rays (Aharonian et al. 2008). We also note that, in this case, the intrinsic VHE luminosity of 3C 66A should exceed 10^{47} erg s^{-1}, which is an unusually large value for a BL Lac object (Wagner 2008), also in view of its spectral characteristics (Persic & De Angelis 2008).

3C 66B is a FRI radio galaxy similar to M 87, which has been detected to emit VHE γ-rays (Aharonian et al. 2003, 2006b). Since the distance of 3C 66B is 85.5 Mpc, its intrinsic VHE luminosity would be two to eight times higher than that of M 87 (22.5 Mpc), given the reported variability of M 87 (Aharonian et al. 2006b; Albert et al. 2008b).

As in the case of M 87, there would be several possibilities for the region responsible of the TeV radiation in 3C 66B: the vicinity of the supermassive black hole (Neronov & Aharonian 2007), the unresolved base of the jet (in analogy with blazar emission models; Tavecchio & Ghisellini 2008a), and the resolved jet. Unlike for M 87, we do not observe significant variability in the VHE γ-ray flux and therefore we have no constrains on the size of the emission region. However, as the angle to line of sight is even larger than in M 87 (M 87: 19°, Perlman et al. 2003; 3C 66B: 45°, Giovannini et al. 2001) the resolved jet seems an unlikely site of the emission. On the other hand, the unresolved base of the jet seems a likely candidate for

[31] See also Stecker et al. (2007) for more detailed calculations.

the emission site as it could point with a smaller angle to the line of sight. If the viewing angle is small, blazar-like emission mechanisms cannot be excluded. The orbital motion of 3C 66B shows evidence for a supermassive black hole binary (SMBHB) with a period of 1.05 $\pm$ 0.03 years (Sudou et al. 2003). The SMBHB would likely cause the jet to be helical, and the pointing direction of the unresolved jet could differ significantly from the direction of the resolved jet.

Given the likely association of MAGIC J0223+430 with 3C 66B, our detection would establish radio galaxies as a new class of VHE γ-ray emitting sources. According to Ghisellini et al. (2005), there are eight FRI radio galaxies in the 3CR catalog that should have a higher γ-ray flux at 100 MeV than 3C 66B, but possibly many of these sources are rather weak in the VHE γ-ray band. Further observations of radio galaxies with the Fermi Gamma-ray Space Telescope as well as by ground-based telescopes are needed to further study the γ-ray emission properties of radio galaxies.

We thank the Instituto de Astrofísica de Canarias for the excellent working conditions at the Observatorio del Roque de los Muchachos in La Palma. The support of the German BMBF and MPG, the Italian INFN, and Spanish MCINN is gratefully acknowledged. This work was also supported by ETH Research Grant TH 34/043, by the Polish MNiSzW Grant N N203 390834, and by the YIP of the Helmholtz Gemeinschaft.

REFERENCES

Aharonian, F. A., Khangulyan, D., & Costamante, L. 2008, MNRAS, 387, 1206
Aharonian, F., et al. 2000, A&A, 353, 847
Aharonian, F., et al. 2003, A&A, 403, 1
Aharonian, F., et al. 2006a, Nature, 440, 1018
Aharonian, F., et al. 2006b, Science, 314, 1424
Albert, J., et al. 2006, ApJ, 648, 105
Albert, J., et al. 2007a, ApJ, 667, 21
Albert, J., et al. 2007b, Nucl. Instrum. Methods A, 583, 494
Albert, J., et al. 2008a, ApJ, 674, 1037
Albert, J., et al. 2008b, ApJ, 685, L23
Albert, J., et al. 2008c, Nucl. Instrum. Methods A, 588, 424
Albert, J., et al. 2008d, Nucl. Instrum. Methods A, 594, 407
Aliu, E., et al. 2009, Astropart. Phys., 30, 293
Bloom, S. D., & Marscher, A. P. 1996, ApJ, 461, 657
Bramel, D. A., et al. 2005, ApJ, 629, 108
Bretz, T., Dorner, D., Wagner, R. M., & Sawallisch, P. 2009, Astropart. Phys., in press (arXiv:0810.4593)
Dermer, C., & Schlickeiser, R. 1993, ApJ, 416, 458
Finke, J. D., Shileds, J. C., Böttcher, M., & Basu, S. 2008, A&A, 477, 513
Fomin, V. P., Stepanian, A., Lamb, R. C., Lewis, D. A., Punch, M., & Weekes, T. C. 1994, Astropart. Phys., 2, 137
Ghisellini, G., Tavecchio, F., & Chiaberge, M. 2005, A&A, 432, 401
Giovannini, G., Cotton, W. D., Feretti, L., Lara, L., & Venturi, T. 2001, ApJ, 552, 508
Gould, R. J., & Schréder, G. P. 1967, Phys. Rev., 155, 1408
Hartman, R. C., et al. 1999, ApJS, 123, 79
Hillas, A. M. 1985, Proc. of the 19th ICRC, La Jolla, 3, 445
Horan, D., et al. 2004, ApJ, 603, 51
Katarzynski, K., Ghisellini, G., Mastichiadis, A., Tavecchio, F., & Maraschi, L. 2006, MNRAS, 368, 52
Kuiper, L., Hermsen, W., Verbunt, F., Thompson, D. J., Stairs, I. H., Lyne, A. J., Strickman, M. S., & Cusumano, G. 2000, A&A, 359, 615
Mannheim, K. 1993, A&A, 269, 67
Maraschi, L., Ghisellini, G., & Celotti, A. 1992, ApJ, 397, 5
Mazin, D., & Raue, M. 2007, A&A, 471, 439
Miller, J. S., French, H. B., & Hawley, S. A. 1978, in Pittsburgh Conf. on BL Lac Objects, ed. A. M. Wolfe (Pittsburgh, PA: Univ. Pittsburgh), 176
Mücke, A., Protheroe, R. J., Engel, R., Rachen, J. P., & Stanev, T. 2003, Astropart. Phys., 18, 593
Neronov, A., & Aharonian, F. 2007, ApJ, 671, 85
Neshpor, Y. I., Stepanyan, A. A., Kalekin, O. P., Fomin, V. P., Chalenko, N. N., & Shitov, V. G. 1998, Astron. Lett., 24, 134
Persic, M., & De Angelis, A. 2008, A&A, 483, 1
Perlman, E. S., Harris, D. E., & Biretta, J. A. 2003, ApJ, 599, L65
Riegel, B., Bretz, T., Dorner, D., & Wagner, R. M. 2005, Proc. of the 29th ICRC, Pune, India, 5, 219
Stecker, F. W., Baring, M. G., & Summerlin, E. J. 2007, ApJ, 667, L29
Stepanyan, A. A., Neshpor, Y. I., Andreeva, N. A., Kalekin, O. P., Zhogolev, N. A., Fomin, V. P., & Shitov, V. G. 2002, Astron. Rep., 46, 634
Stull, M. A., et al. 1975, AJ, 80, 559
Sudou, H., Iguchi, S., Murata, Y., & Taniguchi, Y. 2003, Science, 300, 126
Swordy, S. 2008, Astron. Telegram, 1753, 1
Tavecchio, F., & Ghisellini, G. 2008a, MNRAS, 385, L98
Tavecchio, F., & Ghisellini, G. 2008b, MNRAS, submitted (arXiv:0811.1883)
Teshima, M. 2008, Astron. Telegram, 1500, 1
Tikhonov, A. N., & Arsenin, V. Ja. 1979, Methods of Solution of Ill-posed Problem - M (Moscow: Nauka)
Tosti, G., et al. 2008, Astron. Telegram, 1759, 1
Verbunt, F., et al. 1996, A&A, 311, L9
Wagner, R. M. 2008, MNRAS, 385, 119
Wurtz, R., Stocke, J. T., & Yee, H. K. C. 1996, ApJS, 103, 109